RADIATION-INCLUSIVE KICKMAP ANALYSIS OF INSERTION DEVICES AND MITIGATION STRATEGIES FOR MAX4U

G. Pérez Segurana*, M. Apollonio, J. Bengtsson, M. Muradi, M. Sjöström, H. Tarawneh, P. Tavares, S. Thorin, MAX IV Laboratory, Lund, Sweden

Abstract

Multi-bend achromat lattices allow for the design of extremely low-emittance electron storage rings and are a cornerstone of the performance of storage-ring-based synchrotron light sources. As part of the proposed MAX IV upgrade, MAX4U, we revise the impact of the insertion devices (IDs) on the beam. We extend the kickmap-based tracking analysis by including the effects of radiation and quantify the resilience of the proposed achromats to the different ID settings and configurations. Finally, we present mitigation strategies, both local to each ID and global, that may be tested experimentally in the current MAX IV 3 GeV ring.

INTRODUCTION

The MAX IV 3 GeV storage ring has demonstrated the performance potential of multi-bend achromat (MBA) optics for diffraction-limited synchrotron light sources and provides the operational basis for the MAX 4^{U} upgrade programme [1–5]. The MAX 4^{U} project aims to further improve brightness and coherence while preserving robust operation under a broad range of user configurations, including challenging insertion-device (ID) settings [6]. In this context, a realistic and self-consistent assessment of ID integration is essential, since they can significantly affect the non-linear dynamics.

Previous optics studies for MAX 4^{U} have established linear and non-linear performance trends for candidate achromats and correction strategies [6]. Building on that work, we revisit ID effects using kickmap-based tracking framework [7] extended with $B_{\perp}^{2}$ as developed for the NSLS-II PDR [8,9] to include the radiation effects. The motivation is twofold: (1) to quantify how synchrotron-radiation damping and quantum excitation modify the dynamic response of the lattice; and (2) to compare mitigation options that can be translated into machine-development tests in the present MAX IV ring.

We evaluate local optics re-matching and global tune correction under multi-ID scenarios, with emphasis on operationally realistic constraints on available quadrupole strengths and optics knobs. An overview of the achromat optics, layout and resulting parameters is shown in Fig. 1 and Table 1.

INSERTION DEVICES

Insertion devices constitute a source of optics perturbations. This section summarizes the IDs considered in this work, table 2, and the beam-dynamics mechanisms retained in the tracking model. A broader overview of planned devices is given in Ref. [10]. The Hamiltonian of a planar insertion device can be written as shown in Eq. (1) [8,11]:

$$\langle H \rangle_{\lambda_u} \approx \frac{p_x^2 + p_y^2}{2(1+\delta)} - \frac{y^2}{4\rho_u^2(1+\delta)} + \frac{k_z^2 y^4}{12\rho_u^2(1+\delta)} - \delta + O(p_{x,y}^4), \quad (1)$$

where λ_u is the ID period, ρ_u is the bending radius associated with the peak field, and $k_z = 2\pi/\lambda_u$. The first term corresponds to the linear vertical focusing, while the second represents higher-order component driving the $4\nu_y$ resonance and vertical amplitude dependent tune shift. For elliptically-polarising undulators (EPUs), skew terms introducing coupling are also present. The linear focusing leads to tune shifts and beta-beating, while the non-linear terms can drive resonances and reduce dynamic aperture. These effects are analysed both per device and in combined configurations. The correction strategy developed in the next section therefore separates local restoration around each straight section from global retuning of lattice functions.

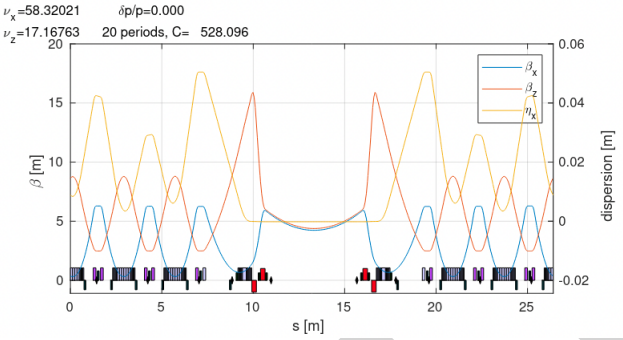

Figure 1: Linear optics of the MAX 4^{U} baseline lattice for one full superperiod shown centered around a long straight. Horizontal beta function β_x (blue), vertical beta function β_y (orange), and horizontal dispersion η_x (yellow) are shown.

Table 1: Key parameters of the MAX 4^{U} baseline lattice used in this study.

Parameter	Symbol	Value
Energy	E	3 GeV
Circumference	C	528 m
Natural emittance	ε_0	65 pm rad
Betatron tunes	Q_x/Q_y	58.32 / 17.17
Chromaticities (corrected)	ξ_x/ξ_y	2 / 2

* gustavo.perez_segurana@maxiv.lu.se

[1] The TomoWISE beamline is not currently present in the MAX IV ring, but will be present at the time of the upgrade to MAX 4^{U}

Table 2: Beamlines with insertion devices considered in this study. Kickmap files generated with RADIA.

Beamline	Period [mm]	Length [m]	Gap [mm]	Phase
MicroMAX	18	2	4.5	-
BioMAX	18	2	4.5	-
ForMAX	17	3	4.5	-
CoSAX	19.3	2	4.5	-
Balder	50	2	4.5	-
TomoWISE[1]	14	2	3.6	-
DanMAX	16	3	4.0	-
NanoMAX	18	2	4.5	-
SoftiMAX	48	4	12.5	15°
HIPPIE	53	4	15.0	15°
Veritas	48	4	12.5	15°

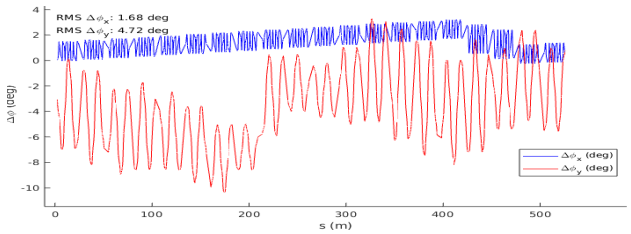

Figure 2: Residual phase beating after local correction and global tune correction.

OPTICS MATCHING

Local correction

A local correction of the optics at each ID can be performed using the flanking quadrupole doublets. For each ID, a pair of solutions exists: overfocusing or underfocusing the beam. These result in different phase advances over the ID and, therefore, different non-linear dynamics. Also, as expected, in cases where the ID is not placed in the centre of the straight, the correction also becomes non-symmetric and hence requires independent powering of all four quadrupoles. The results after a global tune correction restoring the working point are shown in Fig. 2. The local correction is effective in restoring the optics at the ID location; however, asymmetry in the strengths of the IDs leads to residual phase shifts at the sextupoles that impact the dynamics [12].

Global correction

Successful ID integration requires correcting both β and μ, in particular at the locations of the sextupoles. In this section, we implement the method described in [11,13] available in Tracy-3 [14], recently considered for ALS-U [15]. Values of the horizontal and vertical beta-beat and phase-beat are obtained. These, together with the global tunes, form a system of $4N_{\text{sext}} + 2$ equations. Analytical formulae are used for the matrix elements for the linear-optics-response matrix, A, for the resulting system, Eq. (2)

$$\begin{bmatrix} (\Delta\beta_x/\beta_x)_1 \\ \dots \\ (\Delta\beta_x/\beta_x)_{N_{\text{sext}}} \\ (\Delta\beta_y/\beta_y)_1 \\ \dots \\ (\Delta\beta_y/\beta_y)_{N_{\text{sext}}} \\ (\Delta\mu_x)_1 \\ \dots \\ (\Delta\mu_x)_{N_{\text{sext}}} \\ (\Delta\mu_y)_1 \\ \dots \\ (\Delta\mu_y)_{N_{\text{sext}}} \\ \Delta Q_x \\ \Delta Q_y \end{bmatrix} = [A] \cdot \begin{bmatrix} (\Delta K_1)_1 \\ \vdots \\ (\Delta K_1)_{N_{\text{quad}}} \end{bmatrix}. \quad (2)$$

Then, this system of equations is solved using SVD. The correction method depends on knowledge of the beta functions and phases at the sextupoles to be applied to update the lattice model during online error corrections. We also examine the scenario in which the optics at the sextupoles are directly measurable. In the next section, we demonstrate the improved performance of this latter approach, thereby motivating the implementation of such measurements. When applying this correction, we use from each achromat 6 gradients: the two quadrupole doublets in the long straights and the gradient of the outermost reverse bends. The selection of these may be further refined to, for example, reduce the number of power supplies required.

RESULTS

To evaluate the impact of the IDs and the performance of the corrections studied, we compute the DA (dynamic aperture) for the ideal lattice and the different correction setups as shown in Fig. 3. An additional case we present is one with the same machine errors but without IDs. As expected, since to leading order the impact of the IDS is a vertical β-beat the difference between our benchmarks mainly in the vertical plane. We have assumed random girder misalignments (correlated) of: 27 µm horizontal, 21 µm vertical and 157 µrad roll (rms). Additionally, all magnets except dipoles have uncorrelated 4 µm horizontal, 9 µm vertical and 100 µrad roll (rms). The DA is impacted by an artificial aperture restriction in the kick-maps used, while the physical aperture in the long straights housing the IDs spans ±2 mm, the kick-maps only cover ±1.5 mm. These studies will be repeated with kick-maps that cover the full physical aperture currently in preparation.

A summary table showing the β-beating and phase-beating averaged over 20 seeds is shown in table 3. The required quadrupole gradient changes to perform these corrections remain in all cases below ≈1 %.

Finally, we compute on-momentum (Fig. 4) and off-momentum(Fig. 5) frequency maps for a sample seed of

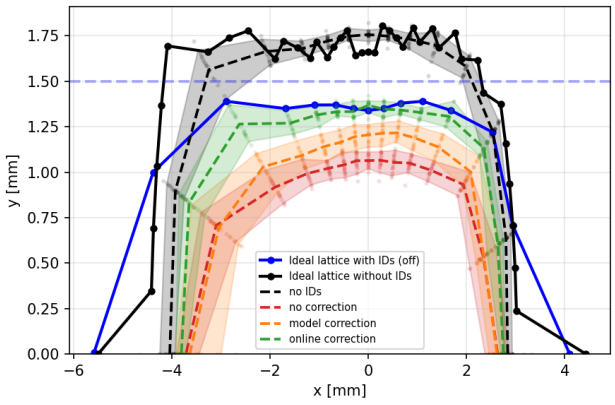

Figure 3: Dynamic Aperture plots for the different configurations evaluated at the centre of a long straight. The ideal lattices with and without IDs are represented by solid lines (blue and black). Shaded band is the 5 to 95 percentile with dashed lines showing the mean. An horizontal line at 1.5 mm is shown to indicate the current limit of the kick-maps used.

Table 3: Average β-beating and phase-beating at the sextupoles at different correction stages.

	$\Delta\beta_x/\beta_x$ [%]	$\Delta\beta_y/\beta_y$ [%]	$\Delta\mu_x$ [°]	$\Delta\mu_y$ [°]
No IDs	0.59(4)	0.80(7)	0.16(4)	0.29(6)
No corr.	3.33(90)	14.58(191)	0.23(4)	1.10(11)
Model	2.70(133)	6.68(368)	35(13)	29(20)
Online	0.89(7)	1.06(8)	0.21(4)	0.51(8)

the online correction scenario. A clear drop in stability is visible when comparing the on-momentum frequency map (same correction applied) with the equivalent lattice without IDs, Fig. 6. Touschek lifetime analysis, using the equilibrium parameters including the IDs ($\epsilon_x = 55$ pm rad, $\sigma_s = 6.0$ mm and $\sigma_\delta = 8.1 \times 10^{-4}$), results in an estimate of 12.4 h for this seed. Although the corrections proposed result in a significant improvement, the lack of compensation from the non-linear effects induced by the IDs must be studied.

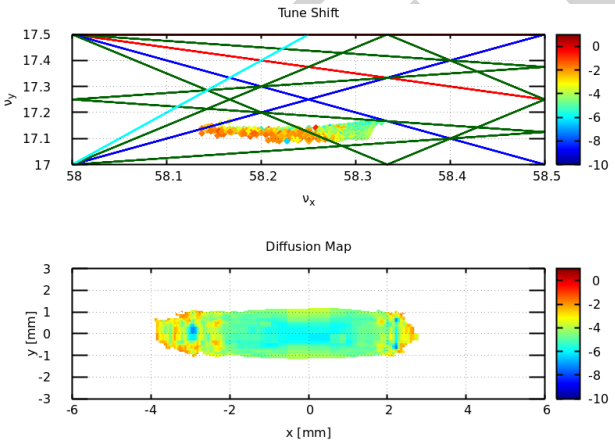

Figure 4: On-momentum frequency map, lattice with IDs and machine errors.

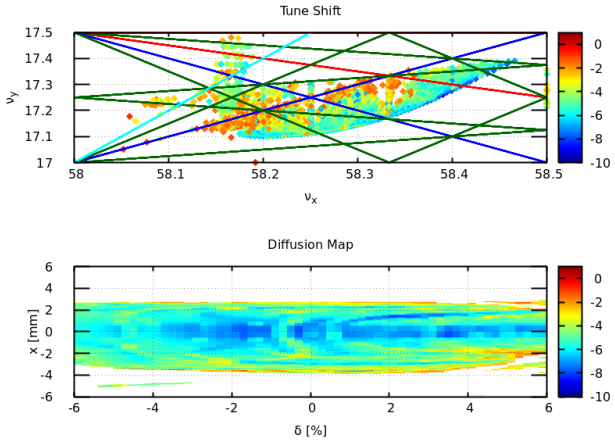

Figure 5: Off-momentum frequency map, lattice with IDs and machine errors.

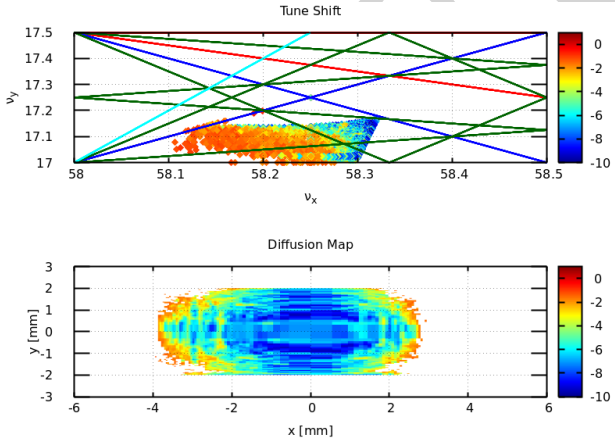

Figure 6: On-momentum frequency map, lattice with machine errors but without IDs.

CONCLUSIONS

Radiation-inclusive tracking shows that insertion devices still perturb the MAX 4^U optics significantly, even though damping mitigates part of the impact. Local correction restores the optics near each ID, but residual phase errors at the sextupoles remain and limit performance.

Global correction using beta and phase matching at the sextupoles gives a clearer improvement in dynamic aperture and frequency-map behaviour. We conclude that accurate optics knowledge, and measurements at the sextupoles, are important for robust operation in MAX 4^U and further studies on the specific implementation of this compensation method for MAX 4^U will be carried out.

REFERENCES

[1] S. C. Leemann *et al.*, "Beam dynamics and expected performance of sweden's new storage-ring light source: MAX IV", *Phys. Rev. Spec. Top. Accel. Beams*, vol. 12, p. 120701, 2009. doi:10.1103/PhysRevSTAB.12.120701

[2] N. Martensson and M. Eriksson, "The saga of MAX IV, the first multi-bend achromat synchrotron light source", *Nucl. Instrum. Methods Phys. Res. A*, vol. 907, pp. 97–104, Nov.

2018. doi:10.1016/j.nima.2018.03.018

[3] M. Apollonio *et al.*, "Beam Dynamics Studies for the MAX 4^U lattices", presented at IPAC'26, Deauville, France, May 2026, paper THP2115, this conference,

[4] E. Al-Dmour *et al.*, "MAX 4^U, an upgrade of the MAX IV 3 GeV ring", presented at IPAC'26, Deauville, France, May 2026, paper THI2M01, this conference,

[5] A. Dixon *et al.*, "Off-phase injection simulations for MAX 4^U", presented at IPAC'26, Deauville, France, May 2026, paper THP2049, this conference,

[6] "MAX 4^U Conceptual Design Report", MAX IV Laboratory, Technical Report, 2025. https://www.maxiv.lu.se/beamlines-accelerators/max-4u/

[7] P. Elleaume, "A New Approach to the Electron Beam Dynamics in Undulators and Wigglers", in *Proc. EPAC'92*, Berlin, Germany, Mar. 1992, pp. 661–664.

[8] J. Bengtsson, "NSLS-II: Robust Dynamic Aperture", Office of Scientific and Technical Information (OSTI), Technical Report, Jan. 2006. doi:10.2172/1525415

[9] "NSLS-II Preliminary Design Report", Brookhaven National Laboratory, United States, Technical Report, Nov. 2007. doi:10.2172/1010602

[10] H. Tarawneh, M. Holz, and M. Muradi, "Upcoming Insertion Devices at MAX IV Facility", presented at IPAC'26, Deauville, France, May 2026, paper THP2155, this conference,

[11] T. V. Shaftan, J. Bengtsson, and S. L. Kramer, "Control of Dynamic Aperture with Insertion Devices", in *Proc. EPAC'06*, Edinburgh, UK, paper THPLS091, pp. 3490–3492, Jul. 2006.

[12] J. Feikes and G. Wuestefeld, "Lifetime Reduction due to Insertion Devices at BESSYII", in *Proc. PAC'03*, Portland, OR, USA, May 2003, pp. 845–847. doi:10.1109/PAC.2003.1289497

[13] J. Bengtsson and E. Forest, "Global matching of the normalized ring", in *AIP Conference Proceedings*, vol. 255, pp. 229–233, 1992. doi:10.1063/1.42301

[14] J. Bengtsson, Tracy 3.5, 2015. https://github.com/jbengtsson/tracy-3.5/

[15] T. Hellert, C. Steier, and M. Venturini, "Lattice correction and commissioning simulation of the advanced light source upgrade storage ring", *Phys. Rev. Accel. Beams*, vol. 25, no. 11, Nov. 2022. doi:10.1103/physrevaccelbeams.25.110701